Carbohydrate Research 487 (2020) 107894

Contents lists available at ScienceDirect

Carbohydrate Research

journal homepage: www.elsevier.com/locate/carres

New *N*-ribosides and *N*-mannosides of rhodanine derivatives with anticancer activity on leukemia cell line: Design, synthesis, DFT and molecular modelling studies

Ahmed I. Khodair[a,*], Mohamed K. Awad[b], Jean-Pierre Gesson[c], Yaseen A.M.M. Elshaier[d,**]

[a] Chemistry Department, Faculty Science, Kafrelsheikh University, 33516, Kafrelsheikh, Egypt
[b] Theoretical Applied Chemistry Unit (TACU), Chemistry Department, Faculty of Science, Tanta University, Tanta, Egypt
[c] Laboratoire Synthèse et Réactivité des Substances Naturelles, Université de Poitiers, CNRS-UMR 6514, 40 Avenue Du Recteur Pineau, Poitiers F, 86022, France
[d] Organic and Medicinal Chemistry Department, Faculty of Pharmacy, University of Sadat City, 32958, Menoufia, Egypt

ARTICLE INFO

Keywords:
Rhodanine
Thiazolidinones
Antileukemic activity
ROCS analysis
Molecular modelling
DFT calculations

ABSTRACT

N-ribosylation and *N*-mannosylation compounds have a great role in compounds activity as anticancer. The reaction of 2-thioxo-4-thiazolidinone (rhodanine) derivatives, as aglycon part, was done with ribofuranose and mannopyranose sugars (glycone part) followed by deacetylation without cleavage of the rhodanine under acidic medium. Conformational analysis has been studied using NMR methods (2D, DQF-COSY, HMQC and HMBC). All final the new deprotected nucleosides were screened against leukemia 1210, and were found to be considerably less potent (Ic50% 1.4–10.6 μM) than doxorubicin (Ic50% 0.02 μM). Compounds **10d** and **10e** which contain ribose moiety have better activity than those with mannose sugar. DFT calculations with B3LYP/6-31 + G (d) level were used to analyze the electronic and geometric characteristics deduced from the stable structure of the compounds. The principal quantum chemical descriptors showed a good correlation with the experimental observations. Rapid Overlay Comparison Similarity (ROCS) study was operated to explain the compounds similarity and to figure out the most important pharmacophoric features.

1. Introduction

In the recent past, tremendous efforts have been made to develop some heterocyclic small molecules as potent anticancer agents. 2-Thioxo-4-thiazolidinone is one of the privileged scaffolds in drug discovery [1–7] and its derivatives have been proven to be attractive compounds due to their outstanding biological activities as anticonvulsant, antibacterial, antiviral, Hepatitis C Virus (HCV) protease and antidiabetic agents [8–14]. Recently, substituted 2-thioxo-4-thiazolidinones as rhodanine were investigated for tumor aggregation inhibitor [15–17]. In this context, heterocyclic molecules containing thiazolidine nucleus such as rhodanine and its bioisostere 2,4-thiazolidinedione (TZD) [18,19] derivatives have exhibited a broad spectrum of anticancer activity [19,20], Fig. 1. TZDs are implicated in cancer development, progression, and metastasis, as Raf/MEK/extracellular signal-regulated kinase (ERK), Wnt signal transduction pathways [21] and peroxisome proliferator activated receptors. GSK1059615 is a novel, ATP-competitive, and reversible PI3Ks inhibitor, Fig. 1 [20,22]. This drug candidate contains thiazolidinone ring linked to pyridinylquinoline through ethene part, Fig. 1. In the same rational, 5-benzilidene-3-ethyl rhodanine (BTR-1) was reported to have wide spectrum anticancer activities with an IC50 value of < 10 μM. BTR-1 contains rhodanine ring linked to arylidine system, Fig. 1 [20]. However, despite these activities, a highly active therapeutic compound from this class is yet to be explored as anticancer agents with less side effects and more potency. Glycosides of structurally similar heterocyclic systems have been reported before [23–27]. In the last few decades, computational chemistry has progressed from a rarity to become a full partner with an experiment in the investigation of organic and biochemical structures and reactions. Computations have become essential to elucidate structures, properties of molecules, mechanisms and selectivity of reaction [28]. The density functional theory (DFT) is one of the most popular theoretical methods used in calculating a great variety of molecular properties such as molecular structures, vibrational frequencies, chemical shifts, non-linear optical (NLO) effects, natural bond orbital (NBO) analysis, molecular electrostatic potential, frontier molecular

* Corresponding author.
** Corresponding author.
E-mail addresses: khodair2020@yahoo.com (A.I. Khodair), yaseen.elshaier@fop.usc.edu.eg (Y.A.M.M. Elshaier).

https://doi.org/10.1016/j.carres.2019.107894
Received 27 August 2019; Received in revised form 10 December 2019; Accepted 13 December 2019
Available online 14 December 2019
0008-6215/

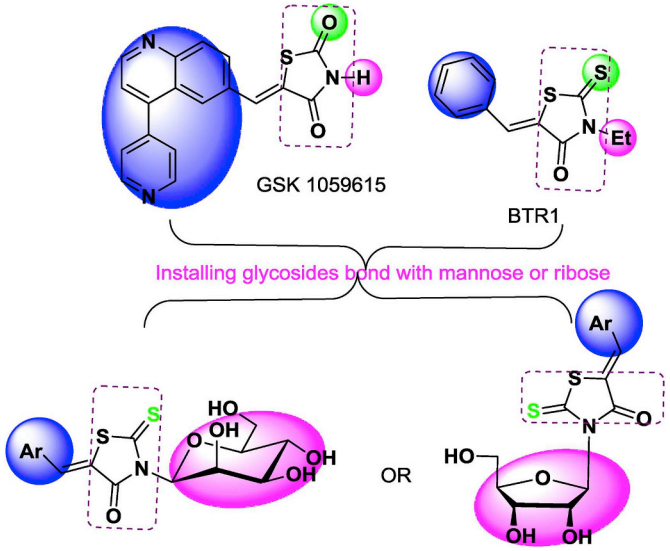

Fig. 1. Potential rhodinine derivatives with anticancer activity and our designed strategy.

orbitals and thermodynamic properties [29–32]. In continuation of our work on the synthesis of novel nucleosides as potential antiviral, antitumor agents and keeping in mind the biological significance of 2-thioxo-4-thiazolidinones [33–36]. We hereby report the synthesis, antitumor screening and spectroscopy analysis of a series of *N*- ribosylated and *N*- mannosylated bearing 2-thioxo-4-thiazolidinone bases. Additionally, we performed the density functional theory to study the effect of the molecular and electronic structure changes on the biological activity of the investigated compounds. ROCS study was operated to figure out the important features in our compounds and explain their 3D-QSAR. The design strategy, as showed in Fig. 1, was elaborated through the following modifications: replacement of arylidine ring by substituted arylidine ring; using rhodanine ring as in BTR-1 and finally, installing sugar moiety to improve drug pharmacokinetics.

2. Results and discussion

The present work describes the synthesis of new series of 5-((*Z*)-arylidene)-3-(2′,3′,5′-tri-*O*-acetyl-β-D-ribofuranosyl)-2-thioxo-4-thiazolidinones (**8a-f**), 5-((*Z*)-arylidene)-3-(β-D-ribofuranosyl)-2-thioxo-4-thiazolidinones (**10a-f**), 5-((*Z*)-arylidene)-3-(2′,3′,4′,6′-tetra-*O*-acetyl-β-D-mannopyranos-yl)-2-thioxo-4-thiazolidinones (**13a-c**) and 5-((*Z*)-arylidene)-3-(β-D-mannopyranosyl)-2-thioxo-4-thiazolidinones (**14a,b**) *via* new synthetic strategies. The silylation of the nucleoside base **1** was accomplished with bis(trimethylsilyl)acetamide (BSA) in anhydrous MeCN at 70–80 °C, and furnished the trimethylsilylated derivative **2**. Derivative **2** was condensed, devised by Vorbrüggen et al. [37], with 1,2,3,5-tetra-*O*-acetyl-β-D-ribofuranose (**3**) in the presence of trimethylsilyl trifluoromethanesulfonate (TMSOTf) as a catalyst at 70–80 °C for 60 min. The protected nucleoside **4** was isolated by silica gel column chromatography in 77% yield. On the other hand and under the same above conditions, the nucleoside bases **6a-f**, were prepared form the direct condensation of **1** with the appropriate aromatic aldehydes (**5a-f**) according to our previous reported procedure [38]. Silylation of nucleoside **6a-f** with BSA affords the trimethylsilylated derivatives **7a-f** which were coupled directly with **3** to give the protected ribonucleosides **8a-f** in high yields. The structures of **4** and **8a-f** were established and confirmed by elemental analyses and spectral data (IR, ^{1}H NMR, ^{13}C NMR and MS). The absence of signal for NH and the presence of signal for the thiocarbonyl group at ν_{max} 1210-1240 cm^{-1} were characterized the IR absorption spectra of **4** and **8a-f**. The proton spin systems were identified from DQF-COSY [39] spectra. The anomeric coupling constants of **4** is a typical for the β-configurated ribofuranoses ($J_{1',2'}$ = 3.1 Hz). The rotating from nuclear overhauser effect (NOE) [40–42] between 1′-H at δ_H 6.58 and 4′-H is an additional proof for β-configuration, and these data are in agreement with those reported earlier by Gosselin et al. [43] The ribosylation occurred at the *N*-site of the 2-thioxo-4-thiazolidinone **(1)**. This was also visible in the HMBC spectrum where the anomeric proton of **4** showed cross peak to C-4 (only one rotator about the ribosidic linkage was observed), and no such correlation to C-5 was shown, indicating for the *N*-ribosylation and not the *S*-ribosylation. Protons bearing carbon were detected in HMQC spectra [44]. The ^{1}H NMR ($CDCl_3$) spectrum of compound **8a** showed a singlet at δ_H 7.69 ppm assigned to the vinyl proton, indicating the presence of a *Z*-configuration for the exocyclic double bond. This is in agreement with the ^{1}H NMR ($CDCl_3$) spectrum of 5-((*Z*)-benzylidene)-3-methyl-2-thioxo-4-thiazolidinone whose vinyl proton appears at δ_H 7.75 ppm [45]. While, the anomeric proton appears as a doublet at δ_H 6.58 ppm ($J_{1',2'}$ = 3.1 Hz), indicating the presence of the β-D-ribofuranose moiety [46]. The ^{13}C NMR ($CDCl_3$) spectrum of **8a** showed a singlet at δ_C 166.4 and 193.1 ppm assigned to the carbonyl at C-4 and the thiocarbonyl group at C-2, respectively. These data are also in agreement with the ^{13}C NMR ($CDCl_3$) spectrum of 5-((Z)-hexylidene-4-oxo-2-thioxothiazolidinyl)-acetic acid [47], since the carbonyl at C-4 appears at δ_c 165.7 ppm and the thiocarbonyl group at C-2 appears at δ_C 194.8 ppm, indicating the presence of *N*-ribosylation. As a chemical evidence for the existence of the *N*-ribosides - not *S*-ribosides, the removal of the acetyl groups in the acetylated nucleosides **4** and **8a-f** were accomplished with concentrated hydrochloric acid in methanol at 50 °C and furnished the corresponding free nucleosides **9** and **10a-f**, respectively. The protected nucleoside **8a** and the deprotected nucleoside **10a** were independently synthesized through another pathway in quantitative yields *via* the condensation of **4** and **9**, respectively, with the benzaldehyde (**5a**) in anhydrous ethanol in the presence of anhydrous morpholine at room temperature (Scheme 1).

This series was extended with more sugar moieties such as the peracetylated mannosyl bromide [48] bearing the 2-thioxo-4-thiazolidinones precursors to examine their potential biological activity. Treatment of **6a,b,e** with 1.1 equivalents of NaH in anhydrous acetonitrile furnished the sodium salts of 5-((*Z*)-arylidene)-2-thioxo-4-thiazolidinones (**11a-c**), which in turn were treated with 2,3,4,6-tetra-*O*-acetyl-α-D-mannopyranosyl bromide (**12**) to afford protected mannonucleosides **13a-c**. Removal of the acetyl groups from the glycon moiety of **13a,b** with a solution of conc. HCl/MeOH at 50 °C for 2 h furnished 5-((*Z*)-arylidene)-3-(β-D-mannopyranosyl)-2-thioxo-4-thiazolidinones (**14a,b**), indicating the presence of *N*-mannosylation. The structures of **13a-c** and **14a,b** were established and confirmed by elemental analyses and spectral data (IR, ^{1}H NMR, ^{13}C NMR and MS). The mass spectrum of **13b** showed a molecular ion peak at *m/z* 581, while the ^{1}H NMR ($CDCl_3$) spectrum of compound **13b** showed a singlet at δ_H 7.68 ppm assigned to the vinyl proton, indicating the presence of a *Z*-configuration for the exocyclic double bond. This is in agreement with the ^{1}H NMR (DMSO-d_6) spectrum of **6b** whose vinyl proton appears at δ_H 7.63 ppm [38]. While, the anomeric proton appears as a doublet at δ_H 6.35 ppm ($J_{1',2'}$ = 9.4 Hz), indicating the presence of the β-D-mannopyranose moiety [49]. The ^{13}C NMR ($CDCl_3$) spectrum of **13b** showed a singlet at δ_C 166.1 and 194.2 ppm assigned to the carbonyl at C-4 and the thiocarbonyl group at C-2, respectively. These data are also in agreement with the ^{13}C NMR (DMSO-d_6) spectrum of **6b**, since the carbonyl at C-4 appears at δ_c 169.7 ppm and the thiocarbonyl group at C-2 appears at δ_C 196.0 ppm [38], indicating the presence of *N*-mannosylation (Scheme 2). Furthermore, the heteronuclear spectra (HMQC, DFQ-COSY) of **14a,b** showed $^3J_{C,H}$ correlation between C-4 and 1′-H, which is an additional proof for *N*-mannosylation.

3. Biological screening

The target compounds **10a-f** and **14a-b** were subjected to anticancer

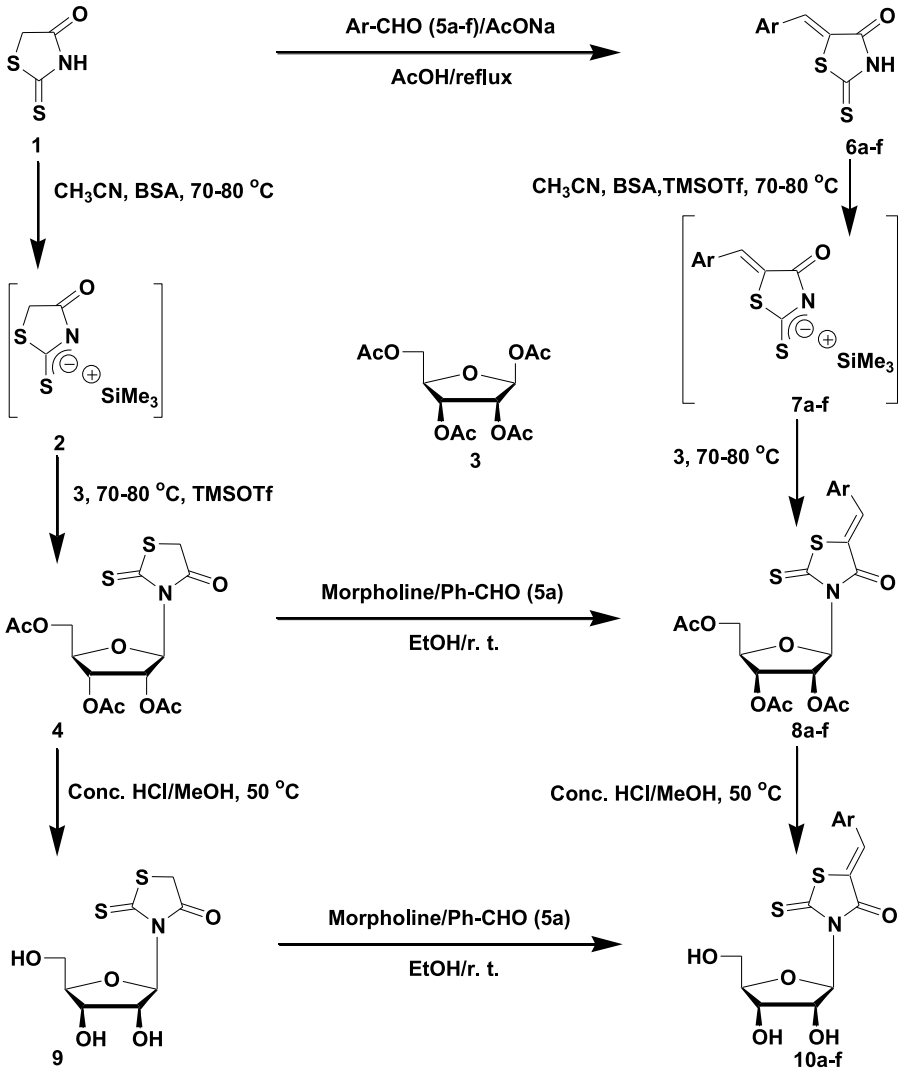

5-10	Ar	5-10	Ar
a	C_6H_5	**d**	2-HO-3-$MeOC_6H_3$
b	4-$MeOC_6H_4$	**e**	2-Thienyl
c	2,4-$Cl_2C_6H_3$	**f**	2-Furyl

Scheme 1. Synthesis of the target compounds **9** and **10a-f**.

against leukemia-1210 using reported method [50]. The Ic50% for all compounds was determined and calculated using doxorubicin as standards, Table 1. All compounds exhibited Ic50% in the range 1.4–12.0 μM in comparison to the standard drug doxorubicin (Ic50% 0.02 μM). Compounds **14a** and **14b** were better in activity (Ic50% = 4.5, 2.3 μM, respectively) than their analogs **10a**, and **10b** (Ic50% = 12.0, 5.2 μM, respectively) indicating that mannose moiety improved the activity rather than ribose ring. Among the ribosyl derivatives, compound **10d** was the most potent one (Ic50% = 1.4 μM) then **10e** (Ic50% = 1.6 μM) followed by **10b** and **10f** (Ic50% = 5.2, 6.3 μM respectively). Finally, compounds **10c**, and **10a** were the least derivatives in activity (Ic50% = 10.6, 12.0 μM, respectively). This pattern indicating presence of electron with drawing group capable for formation of hydrogen bond enhance the compounds activity. Moreover, these values of compounds describe that the aryl ring has a role in activity than the sugar part.

General screening showed that mannosyl series is more active but among all compounds, the ribosyl compounds are more potent. And according to drug discovery strategy, if we will go to synthesize new derivatives and continue in this project, we will focus on ribosyl derivatives not mannosyl derivatives.

4. Qantum chemical calculations

The quantum chemical methods and molecular modelling techniques are able to define a large number of molecular quantities characterizing the reactivity, shape, and binding properties of a complete molecule as well as of molecular fragments and substituents. Quantum chemical calculations were performed to investigate the effect of structural parameters on the biological activity of some investigated compounds. The optimized molecular structures with minimum energies obtained from the calculations of the investigated compounds are shown in Fig. 2.

We started our calculations to make a comparison between *Z*- and *E*-forms for nucleosides and many sides and the calculations showed that the nucleosides and manosides are more stable in the *Z*-form than *E*-form, by about 0.012 au. Also, it was shown from the calculations that they are in β-forms with higher stability than α-form by about 0.008 au, which is in a good agreement with the experimental observations. So, we performed DFT calculations on the stable structures of *Z*-nucleosides

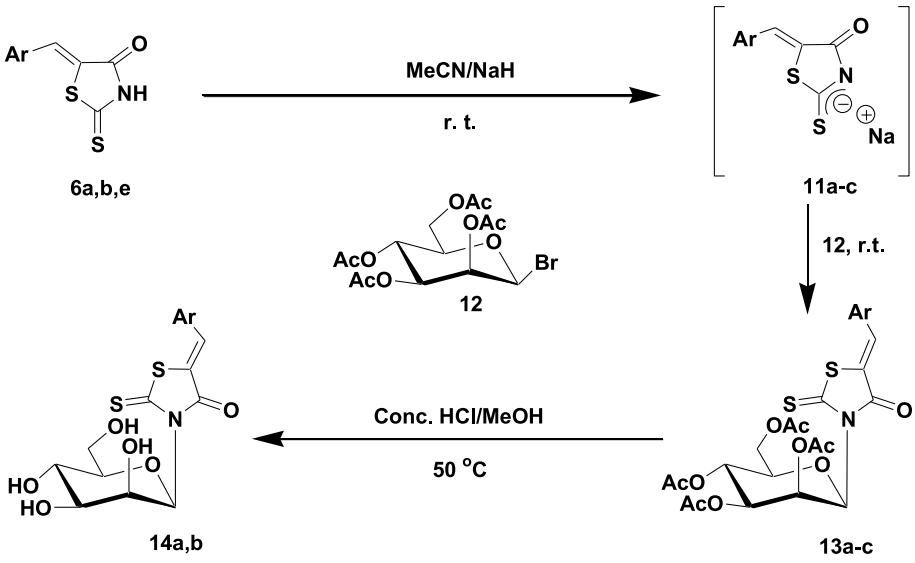

11-14	Ar
a	C_6H_5
b	4-$MeOC_6H_4$
c	2-Thienyl

Scheme 2. Synthesis of the target compounds **13a-c** and **14a,b**.

Table 1
Antitumor activity of 5-((*Z*)-arylidene)-3-(β-D-ribofuranosyl)-2-thioxo-4-thiazolidinones (**10a-f**), and 5-((*Z*)-arylidene)-3-(β-D-mannopyranosyl)-2-thioxo-4-thiazolidinones (**14a,b**) against leukemia-1210.

Compound	Ar	IC_{50}[a] (μM) cellules L-1210
10a	C_6H_5	12
10b	4-$MeOC_6H_4$	5.2
10c	2,4-$Cl_2C_6H_3$	10.6
10d	2-HO-3-$MeOC_6H_3$	1.4
10e	2-Thienyl	1.6
10f	2-Furyl	6.3
14a	C_6H_5	4.5
14b	4-$MeOC_6H_4$	2.3
Doxorubicin		0.02

[a] 50% Inhibitory concentration: molar concentration of compound that cause 50% inhibition for cell growth.

and manosides in the β –forms.

The experimental data showed that the presence of dichloro-substituent at the phenyl moiety of the nucleoside, compound **10c**, showed a low biological activity. Surprisingly, the calculations showed that the dichloro-substituent increases the energy of HOMO (−4.262 eV), which is the donor part of the molecule, increases the softness, decreasing the energy gap between HOMO-LUMO (2.345 eV), which is probably more favourable for the reactivity towards the enzyme, the decreasing of the chemical potential, electronegativity and electrophilicity mean increasing the reactivity of the molecule and accordingly increases the biological activity, which is in contradictory with the experimental observations, Table 1.

The presence of 2-hydroxy-3-methoxy, compound **10d**, and thienyl substituent, compound **10e**, in the α-position of the vinyl moiety of the nucleosides compounds showed a higher biological activity than that for the rest of the investigated compounds, which could be explained from the calculated quantum chemical parameters. The calculations showed that the presence of 2-hydroxy-2-methoxy and thienyl substituents, compounds **10d** and **10e**, decrease the energy of the LUMO (−3.159 and −3.012 eV), respectively, which means that these compounds could react as electrophiles (electron acceptor), Table 2. The electrophilicity is the descriptor of reactivity and is sufficient to describe the toxicity of the molecules. It also provides the direct relationship between the rates of reactions and the ability to identify the function or capacity of an electrophile and the electrophilic power of the compounds. It was shown from the calculations that the compounds 10d and 10e have high electrophilicity indices (6.908 and 6.509 eV), respectively, which probably enhance their biological activities and agree well with the experimental observations.

Also, experimentally, the unsubstituted phenyl moiety, compound **10a**, has the lowest biological activity amongst the nucleosides compounds, which could be explained from the calculated quantum chemical parameters. The calculations showed that the unsubstituted phenyl moiety decreases the energy of the HOMO, the dipole moment and electrophilicity index while increases the energy gap which means decreasing the reactivity of compound 10a and accordingly decreases its biological activity. This is in a good agreement with the experimental data.

It was found from the calculations that the many side compounds, **14a,b** are less reactive than the nucleoside compounds **10d,e** which could be shown from the decreasing of the HOMO energies (−6.615,-6.462 eV), respectively, and increasing the LUMO energies (−2.662,-2.498 eV), respectively, Table 1, which is in a good agreement with the experimental observations. Also, increasing the energy gap between HOMO-LUMO of manosides (3.953, 3.964 eV), respectively, leads to increase its stability and accordingly decreasing its biological activity. Also, it has lower softness (0.506 and 0.505 eV^{-1}), respectively, and electrophilicity values (5.443, 5.063), respectively, than those of nucleosides which are probably responsible for the decreasing its biological activity.

5. Frontier molecular orbitals

The HOMO and LUMO levels are very common quantum chemical parameters which play a role in determining the way the molecule interacts with another molecule. The HOMO and the LUMO levels charge density distribution for the studied molecules are shown in

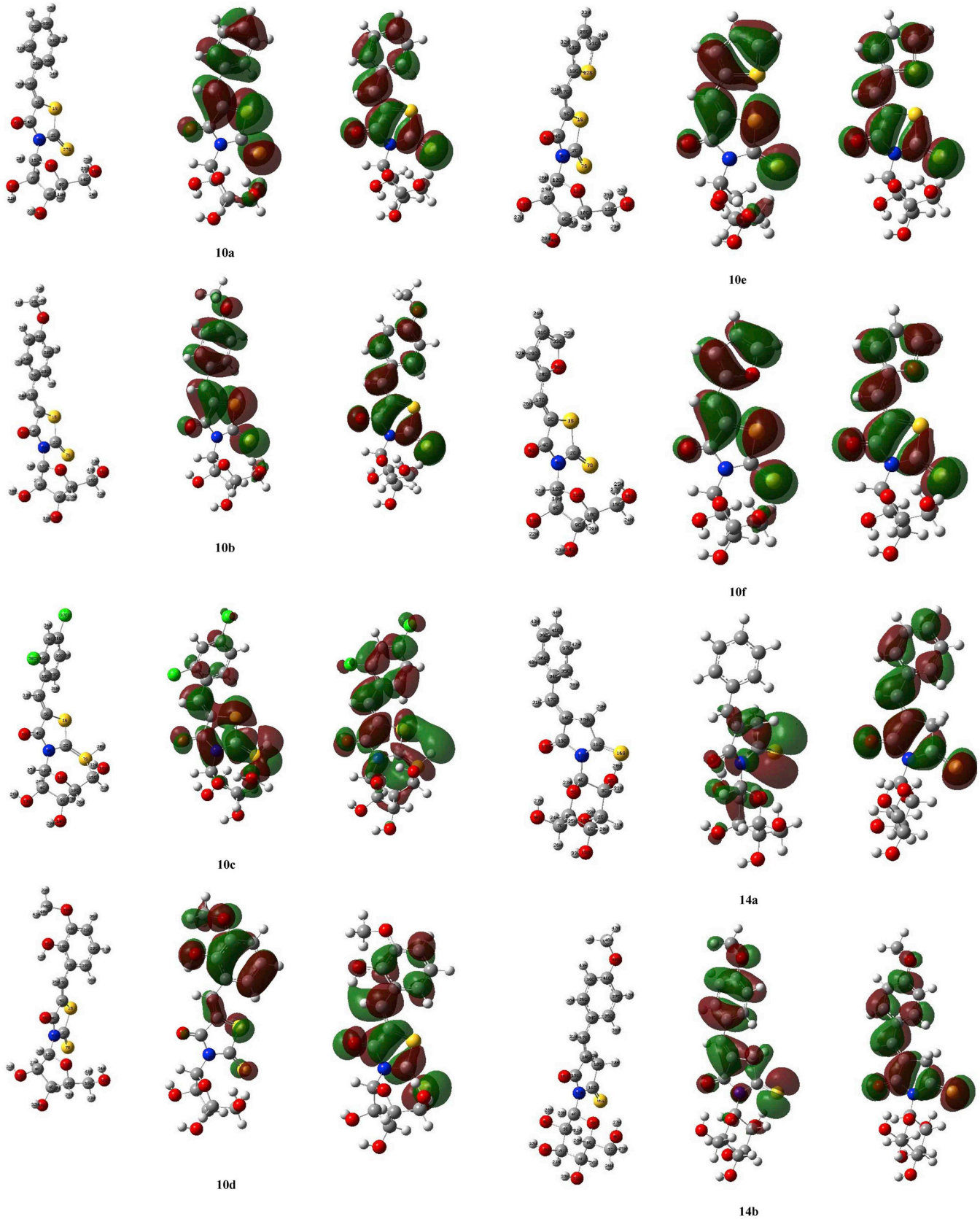

Fig. 2. The optimized molecular structures, charge density distributions (HOMO and LUMO) for the investigated compounds.

Table 2
The calculated quantum chemical parameters obtained from DFT/B3LYP/6-31 + G (d) of the investigated compounds.

Compound	E_{HOMO}(eV)	E_{LUMO}(eV)	ΔE(eV)	DM(D)	IP(eV)	EA(eV)	η(eV)	σ(eV^{-1})	μ(eV)	χ(eV)	ω	Ea.u.	IC_{50}μM
10a	−6.515	−2.991	3.524	4.370	6.515	2.991	1.762	0.568	4.753	−4.753	6.411	−1807.856	12
10b	−6.221	−2.863	3.358	8.371	6.221	2.863	1.679	0.596	4.542	−4.542	6.143	−1922.383	5.2
10c	−4.262	−1.917	2.345	5.919	4.262	1.917	1.173	0.853	3.090	−3.090	4.070	−2726.877	10.6
10d	−6.521	−3.159	3.362	5.513	6.521	3.159	1.681	0.595	4.840	−4.840	6.968	−1997.508	1.4
10e	−6.342	−3.012	3.330	4.873	6.342	3.012	1.665	0.600	4.677	−4.677	6.569	−2128.595	1.6
10f	−6.231	−2.989	3.242	5.338	6.231	2.989	1.621	0.617	4.610	−4.610	6.555	−1805.640	6.3
14a	−6.615	−2.662	3.953	6.974	6.615	2.662	1.977	0.506	4.639	−4.639	5.443	−1563.532	4.5
14b	−6.462	−2.498	3.964	8.405	6.462	2,498	1.982	0.505	4.480	−4.480	5.063	−1678.059	2.3

Fig. 2. It was shown from the investigated compounds that the HOMO levels, which could be reacted as a nucleophile (hydrogen bond acceptor) with the biological target, is mainly localized on the whole molecule except for the trihydroxy six and five membered rings. But in the case of compound **10c**, the dichlorophenyl moiety will slightly contribute in the HOMO level. The LUMO, which could be reacted as a nucleophile (hydrogen bond donor) with the biological target, is mainly delocalized over the whole molecule except for trihydroxy five and six membered rings. The calculations showed that charge transfer may occur from the nucleophilic sites to the electrophilic part of the same molecules.

It is concluded from FMOs that the effect of substituents on the phenyl moiety plays an important role to enhance the affinity of the tested compounds towards the target enzymes.

6. Molecular modelling

6.1. ROCS analysis [51–53]

ROCS is a computational method that used to predict similarity between compounds based on their three dimensional. ROCS analysis requires a) query molecules and here are BTR1 and GSK1059615; b) the database molecules and here are our synthesized compounds. The out puts from ROCs analysis are the overly between the query and database molecules as visualized by vROCS and VIDA applications. The visualization of the query includes different descriptors as shape atoms, shape counter, and color atoms labels. All compounds exhibited high similarity in their ROCs analysis and all of them (except **10a**) illustrated high potency more than query BTR1. It's clear that due to the glycoside moiety, Table 3.

The color shape of query BTR1, illustrated 2 rings, 3 donors, and 2 acceptors, Fig. 3 **(A)**. Compounds **10a**, **10b**, **10c**, **14b** showed high similarity in color and shape to BTR1, Fig. 3 **(B).** Similarly, the standard GSK1059615 has similarity to BTR1 query, Fig. 3 **C.** However, compounds **10e** and **10f** adopted a unique alignment. Both compounds overlay with BTR1 as query in which sugar part acts as ring and 2 acceptors, Fig. **D**. This representation represents the importance of ribose which has quantified more than receptors in addition to their known polarity. Finally, Compound **14a** has a unique and specific pose with BTR1 with BTR. The thiazolidindion ring adopted perpendicular position to same ring with BTR1, Fig. 3 **(E)**.

Considering the Potent inhibitor of PI 3-kinase α (PI3Kα) GSK1059615 as a query, it color shape has 4 rings, 4 acceptors and one donor. The compounds represented high similarity to query GSK1059615 in their color shape and volume. The sugar moiety adopted as a ring and as donor/acceptor descriptor (Fig. 4 B). Both compounds **10d** (Figs. 4C) and **14b** (Fig. 4 D) adopted a certain 3D overlay to GSK1059615.

The second output of ROCs analysis is Tanimoto scores which various aspect of that alignment. The two core scoring methods are Shape Tanimoto (Tanimoto coefficient) and Color Tanimoto. Tanimoto Combo is the sum of those two independent components (Shape and Color Tanimoto). Shape Tanimoto represents the shared volume and mismatch volume and has scale from 0 to 1. Color Tanimoto is the distribution of chemical features in 3D (also scale from 0 to 1), Table 3. The scores are computed and the process is repeated to each conformation of the query molecules (BTR1 and GSK1059615) and each conformation for the database molecule, Table 3. Considering BTR1 as a query, compounds **10a**, **10c** have high Tanimoto Combo score more than GSK1059615 then compounds **10b**, **10d**, **14b**, **10e**, **10f**, and **14a** respectively. However, in the case of GSK1059615 as a query, compound **10d** has high score than BTR1 then compounds **10e**, **10f**, **14a**, **10a**, **10c**, **14b**, and **10b**, respectively.

7. Structure activity relationship

The sugar moieties that linked through glycoside linkage have important roles. Their rules are not only to improve compounds pharmacokinetics but also it participated in compounds features as an important pharmacophore. The ribose derivatives have better in activity more than mannose analogies. This could be due the pose of thiazolidinone thione ring, Fig. 5. In compound **14b**, it is easier to form intramolecular HB which forces the structure to be more rigid that hinder compounds flexibility to adopt a better conformer inside the amino acid clefts in the receptor. Un-substituted aryl ring or presence of EDG (electron donating group) is better than those with EWG (electron withdrawal group) According to Ic50% values and Tanimoto analysis; the designed compounds demonstrated high similarity to BTR1.

Table 3
Tanimoto scores for synthesized compounds, and lead compounds.

Comp.	Tanimoto Combo	Shape Tanimoto	Color Tanimoto	Tanimoto Combo	Shape Tanimoto	Color Tanimoto
GSK1059615	1.004	0.566	0.566	2	1	1
10d	0.905	0.6450	0.260	0.790	0.617	0.173
BTR-I	2	1	1	0.78	0.599	0.181
10e	0.790	0.5560	0.234	0.729	0.579	0.150
10f	0.785	0.5640	0.221	0.713	0.564	0.149
14a	0.656	0.5100	0.145	0.695	0.550	0.145
10a	1.03	0.698	0.333	0.691	0.533	0.158
10c	1.02	0.679	0.333	0.674	0.524	0.150
14b	0.868	0.6130	0.255	0.626	0.496	0.130
10b	0.974	0.667	0.307	0.596	0.460	0.136

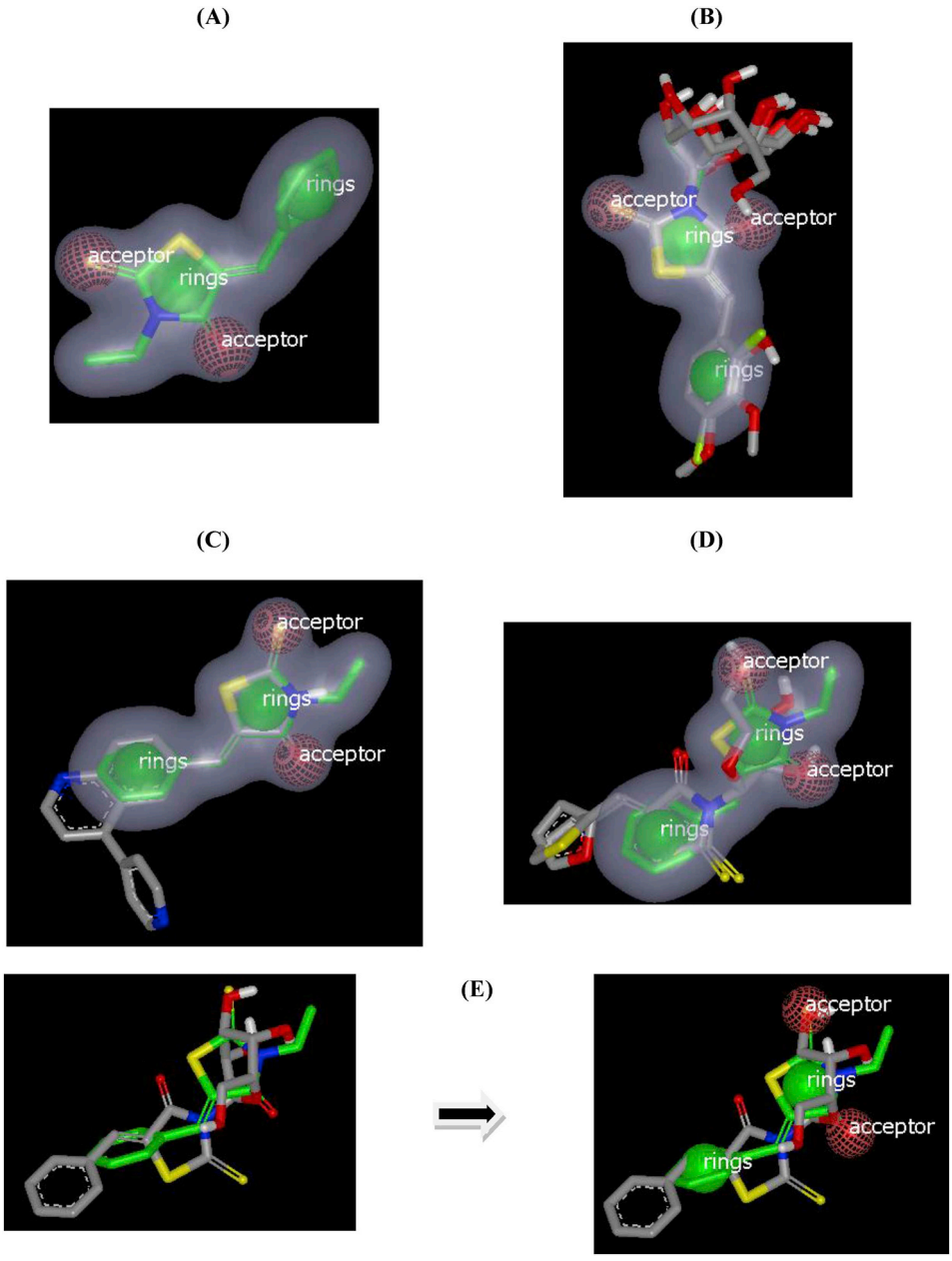

Fig. 3. A) Colour and shape of BTR1 as query; B) Compounds **10a-10c**, and **14b** in color and shape to BTR1; C) Both GSK1059615 and BTR1 (query); D) Compounds **10e** and **10f** with BTR1 as query; E) **14a** with BTR1 with specific pose; **14a** with BTR1 color with specific pose. (For interpretation of the references to color in this figure legend, the reader is referred to the Web version of this article.)

In conclusion, we have described the successful synthesis of ribonucleosides and mannonucleosides of 2-thioxo-4-thiazolidinone derivatives and the confirmation of their most stable conformation by NMR spectroscopy. The ribonucleosides **10a-f** and the mannonucleosides **14a,b** were screened against leukemia-1210, and were found to be considerably less active as compared to doxorubicin (Table 1). The antiviral and the further antitumor activities of the new prepared compounds are under investigation and will be reported in the due time. The nucleoside bases **1** and **6** can be utilized as starting materials for the synthesis of other carbohydrate derivatives as deoxy, amino and azido nucleosides. The electronic and geometric structures were deduced from DFT calculations with B3LYP/6-31 + G (d) level to analyze the stable structure of the compounds. The quantum chemical parameters obtained from the calculations showed a good correlation with the experimental observations. ROCS analysis showed that sugar part is important molecular descriptor. 3D-QSAR showed ribose (furnaose skeleton) is better in activity than mannose (hexoses). The aryl part is better to be with EDG capable to form HB with receptors.

8. Experimental section

General: Melting points were determined on a Büchi apparatus and are uncorrected. TLC was carried out on aluminum sheet silica gel 60 F_{254} (Merck), and detected by short UV light. IR spectra were obtained as potassium bromide pellets using a Pye Unicam spectrometer 1000.^{1}H NMR and ^{13}C NMR spectra were measured on a Bruker Advance DPX 300 MHz spectrometers in DMSO-d_6 or $CDCl_3$ using TMS as internal standard. Chemical shifts are given in ppm and J values in Hz. Analytical data were obtained using a C,H,N Elemental analyzer Carlo Erba 1106. Mass spectra were recorded by EI on a Varian MAT 112 spectrometer and FAB on a Kratos MS spectrometer.

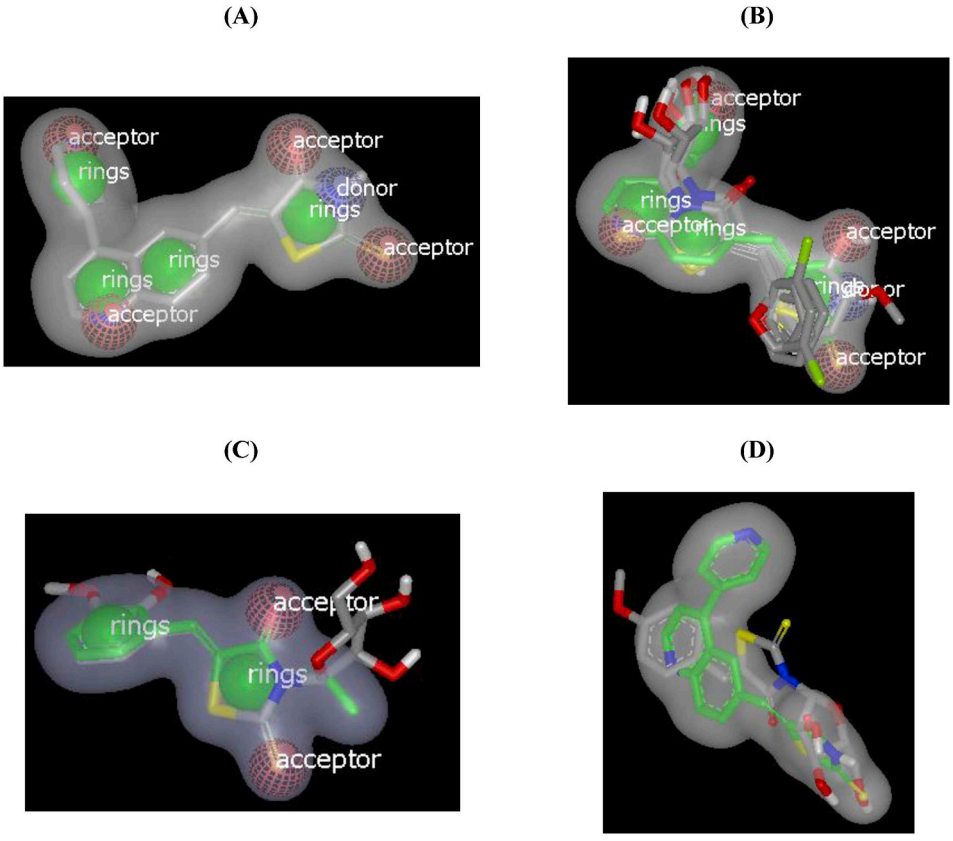

Fig. 4. A) Colour and shape of GSK10596151 as query; B) Color and shape of all compounds except **10b** and **14b**; C) compound**10d**shape with standard volume; D) compound **14b** shape with standard volume. (For interpretation of the references to color in this figure legend, the reader is referred to the Web version of this article.)

8.1. 3-(2′,3′,5′-Tri-O-acetyl-β-D-ribofuranosyl)-2-thioxo-4-thiazolidinone (4)

2-Thioxo-4-thiazolidinone (**1**) (665 mg, 5 mmol) was suspended in anhydrous acetonitrile (25 ml) and BSA (1.25 ml, 5 mmol) was added, and the reaction mixture was heated at 70–80 °C for 30 min. The 1,2,3,.5-tetra-*O*-acetyl-α-D-ribofuranose (**3**) (1.75 g, 5 mmol) dissolved in anhydrous acetonitrile (25 ml) was added to the reaction mixture *via* a cannula. Finally TMSOTf (1.00 ml, 5 mmol) was added, and the reaction mixture was heated at 70–80 °C for 60 min. Saturated $NaHCO_3$ was added to quench the reaction and the resulting mixture extracted with CH_2Cl_2. The combined organic fractions were washed with saturated NaCl solution, dried over $MgSO_4$, filtered, and evaporated under reduced pressure till dryness. The product was purified by flash chromatography (eluent 30–50%, diethyl ether/petroleum ether, 40–60 °C) to afford 3.00 g (77%) of **4** as yellow foams. IR (KBr): *ν* 1746 cm^{-1} (CO), 1238 cm^{-1} (CS); ^1H NMR ($CDCl_3$): *δ* 2.09 (s, 3H, Ac), 2.10 (s, 3H, Ac), 2.11 (s, 3H, Ac), 3.95 (s, 2H, 5-H), 4.19–4.45 (m, 3H, 4′-H, 5′-H, 5″-H), 5.52 (dd, *J* = 6.7, 7.0 Hz, 1H, 3′-H), 5.85 (dd, *J* = 3.3, 6.6 Hz, 1H, 2′-H), 6.40 (d, *J* = 3.2 Hz, 1H, 1′-H); ^{13}C NMR ($CDCl_3$): *δ* 20.74, 20.81, 20.85 (3 Ac), 35.02 (C-5), 63.50 (C-5′), 70.04 (C-3′), 71.26 (C-2′), 80.01 (C-4′), 84.30 (C-1′), 169.98, 170.06, 171.20 (3 Ac), 174.00 (C-4), 202.15 (C-2); MS, *m/z* = 391 (M^+); Anal. Calcd. for $C_{14}H_{17}NO_8S_2$ (391.42): C, 42.96; H, 4.38; N, 3.58. Found: C, 43.17; H, 4.60; N, 3.42.

8.2. 5-((Z)-Arylidene)-3-(2′,3′,5′-tri-O-acetyl-β-D-ribofuranosyl)-2-thioxo-4-thiazolidinone (8a-f)

Method A: General Procedure: 5-((*Z*)-Arylidene)-2-thioxo-4-thiazolidinones (**6a-f**) (5 mmol) were suspended in anhydrous acetonitrile (25 ml) and BSA (1.25 ml, 5 mmol) was added, and the reaction

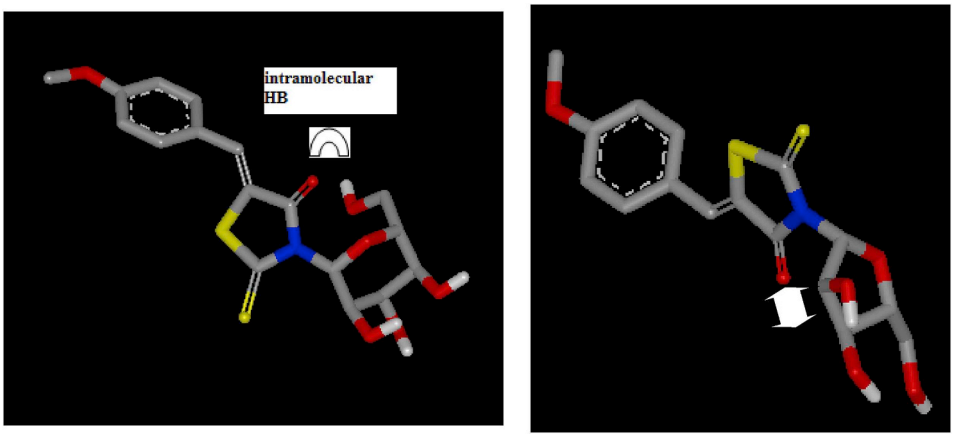

Fig. 5. 3D representation of compounds **14b**, **10b** in which compound **14b** more available to form intrameolecular HB.

mixture was heated at 70–80 °C for 30 min. The 1,2,3,5-tetra-*O*-acetyl-α-D-ribofuranose (**3**) (1.75 g, 5 mmol) dissolved in anhydrous acetonitrile (25 ml) was added to the reaction mixture *via* a cannula. Finally, TMSOTf (1.00 ml, 5 mmol) was added, and the reaction mixture was heated at 70–80 °C for 60 min. Saturated $NaHCO_3$ was added to quench the reaction and the resulting mixture extracted with CH_2Cl_2. The combined organic fractions were washed with saturated NaCl solution, dried over $MgSO_4$, filtered, and evaporated to dryness. The products were purified by flash chromatography (eluent 30–50%, diethyl ether/petroleum ether, 40–60 °C) to afford the title compounds **8a-f** in good yields.

8.3. 5-((Z)-Benzylidene)-3-(2′,3′,5′-tri-O-acetyl-β-D-ribofuranosyl)-2-thioxo-4-thiazolidinone (8a)

Yield 2.00 g (83%); yellow foams; IR (KBr): ν 1748 cm^{-1} (CO), 1232 cm^{-1} (CS); ^1H NMR ($CDCl_3$): δ 2.11 (s, 3H, Ac), 2.12 (s, 3H, Ac), 2.13 (s, 3H, Ac), 4.25 (dd, J = 6.2, 11.7 Hz, 1H, 4′-H), 4.34 (ddd, J = 2.8, 7.3, 10.5 Hz, 1H, 5′-H), 4.53 (dd, J = 3.0, 11.7 Hz, 1H, 5″-H), 5.67 (dd, J = 6.3, 7.0 Hz, 1H, 3′-H), 5.96 (dd, J = 3.2, 6.5 Hz, 1H, 2′-H), 6.58 (d, J = 3.1 Hz, 1H, 1′-H), 7.48 (m, 5H, Ar–H), 7.69 (s, 1H, =CH); ^{13}C NMR ($CDCl_3$): δ 20.26, 20.30, 20.58 (3 Ac), 62.84 (C-5′), 70.10 (C-3′), 71.71 (C-2′), 79.25 (C-4′), 87.65 (C-1′), 121.12 (=CH), 129.24, 130.54, 130.86, 132.92 (C–Ar), 133.69 (C-5), 166.40 (C-4), 169.26, 169.43, 170.44(3 Ac), 193.11 (C-2); MS, m/z = 479 (M^+); Anal. Calcd. for $C_{21}H_{21}NO_8S_2$ (479.53): C, 52.60; H, 4.41; N, 2.92. Found: C, 52.84; H, 4.67; N, 2.80.

8.4. 5-((Z)-4-Methoxybenzylidene)-3-(2′,3′,5′-tri-O-acetyl-β-D-ribofuranosyl)-2-thioxo-4-thiazolidinone (8b)

Yield 2.18 g (86%); yellow solid; mp 87–89 °C; IR (KBr): ν 1746 cm^{-1} (CO), 1230 cm^{-1} (CS); ^1H NMR ($CDCl_3$): δ 2.08 (s, 3H, Ac), 2.10 (s, 3H, CH_3), 2.12 (s, 3H, Ac), 3.87 (s, 3H, OCH_3), 4.21 (dd, J = 6.2, 11.7 Hz, 1H, 4′-H), 4.30 (ddd, J = 2.8, 7.3, 10.5 Hz, 1H, 5′-H), 4.51 (dd, J = 2.8, 11.6 Hz, 1H, 5″-H), 5.66 (dd, J = 6.5, 7.1 Hz, 1H, 3′-H), 5.93 (dd, J = 3.2, 6.5 Hz, 1H, 2′-H), 6.57 (d, J = 2.8 Hz, 1H, 1′-H), 7.00, 7.45 (2d, J = 8.9 Hz, 4H, Ar–H), 7.66 (s, 1H, =CH); ^{13}C NMR ($CDCl_3$): δ 20.51, 20.80 (3 Ac), 55.58 (OCH_3), 63.08 (C-5′), 70.26 (C-3′), 71.96 (C-2′), 79.36 (C-4′), 87.82 (C-1′), 115.03, 118.14, 125.85, 132.93, 134.03, 161.97 (=CH, C–Ar, C-5), 166.76 (C-4), 169.47, 169.65, 170.40 (3 Ac), 193.35 (C-2); MS, m/z = 509 (M^+); Anal. Calcd. for $C_{22}H_{23}NO_9S_2$ (509.55): C, 51.86; H, 4.55; N, 2.75. Found: C, 51.98; H, 4.80; N, 2.62.

8.5. 5-((Z)-2,3-Dichlorobenzylidene)-3-(2′,3′,5′-tri-O-acetyl-β-D-ribofuranosyl)-2-thioxo-4-thiazolidinone (8c)

Yield 2.11 g (77%); yellow oil; IR (KBr): ν 1748 cm^{-1} (CO), 1225 cm^{-1} (CS); ^1H NMR ($CDCl_3$): δ 2.11 (s, 3H, Ac), 2.12 (s, 3H, Ac), 2.13 (s, 3H, Ac), 4.27 (dd, J = 6.2, 11.7 Hz, 1H, 4′-H), 4.32 (ddd, J = 2.8, 7.3, 10.5 Hz, 1H, 5′-H), 4.54 (dd, J = 2.9, 11.9 Hz, 1H, 5″-H), 5.65 (dd, J = 6.2, 6.5 Hz, 1H, 3′-H), 5.93 (dd, J = 3.0, 6.5 Hz, 1H, 2′-H), 6.55 (d, J = 2.9 Hz, 1H, 1′-H), 7.28–7.52 (m, 3H, Ar–H), 7.98 (s, 1H, =CH); ^{13}C NMR ($CDCl_3$): δ 20.45, 20.48, 20.78 (3 Ac), 62.82 (C-5′), 70.07 (C-3′), 71.90 (C-2′), 79.36 (C-4′), 87.90 (C-1′), 124.56 (=CH), 127.92, 128.28, 129.85, 130.02, 130.56, 136.96, 137.23 (C–Ar, C-5), 166.00 (C-4), 169.47, 169.68, 170.67 (3 Ac), 192.32 (C-2); MS, m/z = 548 (M^+); Anal. Calcd. for $C_{21}H_{19}Cl_2NO_8S_2$ (548.41): C, 45.99; H, 3.49; N, 2.55. Found: C, 46.22; H, 3.65; N, 2.38.

8.6. 5-((Z)-2-Hydroxy-3-methoxybenzylidene)-3-(2′,3′,5′-tri-O-acetyl-β-D-ribofuranos-yl)-2-thioxo-4-thiazolidinone (8d)

Yield 1.84 g (70%); yellow foams; IR (KBr): ν 1750 cm^{-1} (CO), 1226 cm^{-1} (CS); ^1H NMR ($CDCl_3$): δ 2.06 (s, 3H, Ac), 2.09 (s, 3H, CH_3), 2.12 (s, 3H, Ac), 3.86 (s, 3H, OCH_3), 4.20 (dd, J = 6.3, 11.6 Hz, 1H, 4′-H), 4.32 (ddd, J = 2.9, 7.2, 10.6 Hz, 1H, 5′-H), 4.54 (dd, J = 2.9, 11.6 Hz, 1H, 5″-H), 5.68 (dd, J = 6.4, 7.1 Hz, 1H, 3′-H), 5.92 (dd, J = 3.1, 6.5 Hz, 1H, 2′-H), 6.58 (d, J = 2.9 Hz, 1H, 1′-H), 6.58 (s, 1H, OH), 7.00, 7.46 (2d, J = 8.50 Hz, 4H, Ar–H), 7.68 (s, 1H, =CH); MS, m/z = 525 (M^+); Anal. Calcd. for $C_{22}H_{23}NO_{10}S_2$ (525.55): C, 50.28; H, 4.41; N, 2.67. Found: C, 50.36; H, 4.62; N, 2.60.

8.7. 5-((Z)-2-Thienylidene)-3-(2′,3′,5′-tri-O-acetyl-β-D-ribofuranosyl)-2-thioxo-4-thiazolidinone (8e)

Yield 2.00 g (82%); yellow foams; IR (KBr): ν 1747 cm^{-1} (CO), 1230 cm^{-1} (CS); ^1H NMR ($CDCl_3$): δ 2.10 (s, 3H, Ac), 2.11 (s, 3H, Ac), 2.12 (s, 3H, Ac), 4.23–4.52 (m, 3H, 4′-H, 5′-H, 5″-H), 5.67 (dd, J = 6.5, 7.0 Hz, 1H, 3′-H), 5.95 (dd, J = 3.0, 7.3 Hz, 1H, 2′-H), 6.55 (d, J = 3.1 Hz, 1H, 1′-H), 7.20 (dd, J = 3.7, 5.0 Hz, 1H, 4″-H), 7.42 (d, J = 3.7 Hz, 1H, 3″-H), 7.74 (d, J = 5.0 Hz, 1H, 5″-H), 7.85 (s, 1H, =CH); ^{13}C NMR ($CDCl_3$): δ 20.69, 20.74, 20.02 (3 Ac), 63.24 (C-5′), 70.44 (C-3′), 72.10 (C-2′), 79.59 (C-4′), 88.11 (C-1′), 119.30 (=CH), 126.42, 129.32, 133.84, 134.75, 137.97 (C–Ar, C-5), 166.52 (C-4), 169.79, 169.86, 170.86 (3 Ac), 192.71 (C-2); MS, m/z = 485 (M^+); Anal. Calcd. for $C_{19}H_{19}NO_8S_3$ (485.55): C, 47.00; H, 3.94; N, 2.88. Found: C, 47.18; H, 4.20; N, 2.67.

8.8. 5-((Z)-2-Furylidene)-3-(2′,3′,5′-tri-O-acetyl-β-D-ribofuranosyl)-2-thioxo-4-thiazolidinone (8f)

Yield 2.00 g (85%); yellow foams; IR (KBr): ν 1748 cm^{-1} (CO), 1238 cm^{-1} (CS); ^1H NMR ($CDCl_3$): δ 2.10 (s, 3H, Ac), 2.11 (s, 3H, Ac), 2.12 (s, 3H, Ac), 4.23–4.52 (m, 3H, 4′-H, 5′-H, 5″-H), 5.67 (t, J = 6.96 Hz, 1H, 3′-H), 5.95 (dd, J = 3.03, 7.32 Hz, 1H, 2′-H), 6.55 (d, J = 3.0 Hz, 1H, 1′-H), 6.68 (dd, J = 3.7, 5.0 Hz, 1H, 4″-H), 7.23 (d, J = 3.7 Hz, 1H, 3″-H), 7.40 (d, J = 5.0 Hz, 1H, 5″-H), 7.85 (s, 1H, =CH); MS, m/z = 469 (M^+); Anal. Calcd. for $C_{19}H_{19}NO_9S_2$ (469.49): C, 48.61; H, 4.08; N, 2.98. Found: C, 48.86; H, 4.35; N, 2.79.

Method B: To a mixture of the protected nucleoside **4** (391 mg, 1 mmol), anhydrous morpholine (0.09 g, 1 mmol) and anhydrous ethanol (10 ml) was added benzaldehyde (0.11 g, 1 mmol). The mixture was stirred until the starting material was consumed (12 h; TLC). The reaction mixture was neutralized with HCl/MeOH. After stirring for 5 min, the solution was evaporated *in vacuo* and the residue was purified by flash chromatography (eluent 30–50%, diethyl ether/petroleum ether, 40–60 °C) to afford 412 mg (86%) of **8a** as yellow solid.

8.9. 3-(β-D-Ribofuranosyl)-2-thioxo-4-thiazolidinone (9)

The protected nucleoside **4** (1 mmol) was suspended in MeOH (15 ml), and concentrated HCl (0.5 ml) was added. The reaction mixture was heated for 2 h at 50 °C. To the resulting solution was added an ion exchange resin (Amberlite IR-120, OH^--form), previously washed with MeOH. After stirring for 5 min, the solution was filtered and evaporated *in vacuo* and the residue was purified by flash chromatography (eluent 0–5%, $CHCl_3$/MeOH) to afford 212 mg (80%) of **9** as pale yellow solid; mp 143–145 °C; IR (KBr): ν 3441 cm^{-1} (OH), 1651 cm^{-1} (CO), 1239 cm^{-1} (CS); ^1H NMR (CD_3OD-d_4): δ 3.49 (s, 2H, 5-H), 3.62 (dd, J = 4.4, 13.3 Hz, 2H, 5′-H, 5″-H), 3.85 (dd, J = 4.1, 14.0 Hz, 1H, 4′-H), 4.07 (dd, J = 5.5, 8.6 Hz, 1H, 3′-H), 5.12 (dd, J = 5.2, 5.3 Hz, 1H, 2′-H), 5.73 (d, J = 5.3 Hz, 1H, 1′-H); ^{13}C NMR (DMSO-d_6): δ 43.51 (C-5), 61.82 (C-5′), 73.02 (C-3′), 81.26 (C-2′), 87.14 (C-4′), 90.12 (C-1′), 174.75 (C-4), 192.87 (C-2); MS, m/z = 265 (M^+); Anal. Calcd. for $C_8H_{11}NO_5S_2$ (265.31): C, 36.22; H, 4.18; N, 5.28. Found: C, 36.46; H, 4.41; N, 5.17.

8.10. 5-((Z)-Arylidene)-3-(β-D-ribofuranosyl)-2-thioxo-4-thiazolidinone (10a-f)

Method A: General Procedure: The protected nucleosides **8a-f** (1 mmol) were suspended in MeOH (15 ml), and concentrated HCl (0.5 ml) was added. The reaction mixture was heated for 2 h at 50 °C. To the resulting solution was added an ion exchange resin (Amberlite IR-120, OH^--form), previously washed with MeOH. After stirring for 5 min, the solution was filtered and evaporated *in vacuo* and the residue was purified by flash chromatography (eluent 0–5%, $CHCl_3$/MeOH) to afford the title compounds **10a-f**.

8.11. 5-((Z)-Benzylidene)-3-(β-D-ribofuranosyl)-2-thioxo-4-thiazolidinone (10a)

Yield 296 mg (84%); yellow solid; mp 170–172 °C; IR (KBr): *ν* 3400 cm^{-1} (OH), 1717 cm^{-1} (CO), 1225 cm^{-1} (CS); ^{1}H NMR (DMSO-d_6): *δ* 3.50 (dd, *J* = 6.3, 11.9 Hz, 1H, 5′-H), 3.65 (dd, *J* = 4.2, 11.9 Hz, 1H, 5″-H), 3.80 (dd, *J* = 4.5, 4.6 Hz, 1H, 4′-H), 4.21 (dd, *J* = 5.8, 5.8 Hz, 1H, 3′-H), 4.75 (m, 2H, 2′-H, 3′-OH), 5.15 (d, *J* = 6.1 Hz, 1H, 5′-OH), 5.36 (d, *J* = 5.1 Hz, 1H, 2′-OH), 6.33 (d, *J* = 3.6 Hz, 1H, 1′-H), 7.50–7.65 (m, 5H, Ar–H), 7.80 (s, 1H, =CH); ^{13}C NMR (DMSO-d_6): *δ* 61.93 (C-5′), 70.30 (C-3′), 70.39 (C-2′), 85.03 (C-4′), 90.17 (C-1′), 121.07 (=CH), 131.55 (C-5), 129.91, 130.97, 133.00, 133.74 (C–Ar), 166.49 (C-4), 195.18 (C-2); MS, *m/z* = 353 (M^+); Anal. Calcd. for $C_{15}H_{15}NO_5S_2$ (353.42): C, 50.98; H, 4.28; N, 3.96. Found: C, 51.30; H, 4.62; N, 3.79.

8.12. 5-((Z)-4-Methoxybenzylidene)-3-(β-D-ribofuranosyl)-2-thioxo-4-thiazolidinone (10b)

8.12.1. Yield 298 mg (78%); yellow solid; mp 178–180 °C; IR (KBr)

ν 3378 cm^{-1} (OH), 1718 cm^{-1} (CO), 1228 cm^{-1} (CS); ^{1}H NMR (DMSO-d_6): *δ* 3.46 (dd, *J* = 6.0, 12.2 Hz, 1H, 5′-H), 3.63 (dd, *J* = 5.3, 11.7 Hz, 1H, 5″-H), 3.80 (dd, *J* = 6.0, 6.3 Hz, 1H, 4′-H), 3.85 (s, 3H, OCH_3), 4.16 (dd, *J* = 6.0, 6.0 Hz, 1H, 3′-H), 4.72 (m, 2H, 2′-H, 3′-OH), 5.12 (d, *J* = 6.2 Hz, 1H, 5′-OH), 5.34 (d, *J* = 5.3 Hz, 1H, 2′-OH), 6.33 (d, *J* = 4.0 Hz, 1H, 1′-H), 7.15, 7.63 (2d, *J* = 8.8 Hz, 4H, Ar–H), 7.78 (s, 1H, =CH); ^{13}C NMR (DMSO-d_6): *δ* 55.87 (OCH_3), 62.06 (C-5′), 70.35 (C-3′), 70.50 (C-2′), 85.19 (C-4′), 90.20 (C-1′), 115.46, 117.65, 125.69, 133.32, 133.84, 161.90 (=CH, C-5, C–Ar), 166.50 (C-4), 194.99 (C-2); MS, *m/z* = 383 (M^+); Anal. Calcd. for $C_{16}H_{17}NO_6S_2$ (383.44): C, 50.12; H, 4.47; N, 3.65. Found: C, 50.36; H, 4.71; N, 3.56.

8.13. 5-((Z)-2,3-Dichlorobenzylidene)-3-(β-D-ribofuranosyl)-2-thioxo-4-thiazolidinone (10c)

Yield 350 mg (83%); yellow solid; mp 137–139 °C; IR (KBr): *ν* 3400 cm^{-1} (OH), 1712 cm^{-1} (CO), 1230 cm^{-1} (CS); ^{1}H NMR (DMSO-d_6 + D_2O): *δ* 3.46 (dd, *J* = 6.4, 11.9 Hz, 1H, 5′-H), 3.64 (dd, *J* = 4.1, 11.9 Hz, 1H, 5″-H), 3.80 (dd, *J* = 6.1, 6.1 Hz, 1H, 4′-H), 4.16 (dd, *J* = 5.8, 5.9 Hz, 1H, 3′-H), 4.69 (dd, *J* = 4.2, 5.6 Hz, 2′-H), 6.26 (d, *J* = 4.0 Hz, 1H, 1′-H), 7.40–7.68 (m, 4H, Ar–H, =CH); ^{13}C NMR (DMSO-d_6): *δ* 61.97 (C-5′), 70.38 (C-3′), 70.42 (C-2′), 85.24 (C-4′), 90.29 (C-1′), 125.33, 126.69, 128.79, 129.97, 130.33, 130.85, 135.97, 136.36 (=CH, C-5, C–Ar), 165.97 (C-4), 194.60 (C-2); MS, *m/z* = 422 (M^+); Anal. Calcd. for $C_{15}H_{13}Cl_2NO_5S_2$ (422.30): C, 42.66; H, 3.10; N, 3.32. Found: C, 42.75; H, 3.48; N, 3.12.

8.14. 5-((Z)-2-Hydroxy-3-methoxybenzylidene)-3-(β-D-ribofuranosyl)-2-thioxo-4-thiazolidinone (10d)

Yield 350 mg (83%), yellow solid mp °C; IR (KBr): *ν* 3400 cm^{-1} (OH), 1718 cm^{-1} (CO) 1225 cm^{-1} (CS); ^{1}H NMR (DMSO-d_6 + D_2O): *δ* 3.44 (dd, *J* = 6.3, 11.9 Hz, 1H, 5′-H), 3.65 (dd, *J* = 4.2, 11.9 Hz, 1H, 5″-H), 3.80 (dd, *J* = 6.0, 6.1 Hz, 1H, 4′-H), 3.87 (s, 3H, OMe), 4.18 (dd, *J* = 5.8, 5.9 Hz, 1H, 3′-H), 4.72 (dd, *J* = 4.2, 5.6 Hz, 2′-H), 6.28 (d, *J* = 4.0 Hz, 1H, 1′-H), 6.86–7.16 (m, 3H, Ar–H), 7.92 (s, 1H, =CH); MS, *m/z* = 399 (M^+); Anal. Calcd. for $C_{16}H_{17}NO_7S_2$ (399.44): C, 48.11; H, 4.29; N, 3.51. Found: C, 48.27; H, 4.55; N, 3.37.

8.15. 5-((Z)-2-Thienylidene)-3-(β-D-ribofuranosyl)-2-thioxo-4-thiazolidinone (10e)

Yield 284 mg (79%), yellow solid; mp 142–144 °C; IR (KBr): *ν* 3400 cm^{-1} (OH), 1707 cm^{-1} (CO), 1224 cm^{-1} (CS); ^{1}H NMR (DMSO-d_6): *δ* 3.46 (dd, *J* = 6.2, 12.1 Hz, 1H, 5′-H), 3.65 (dd, *J* = 4.8, 11.6 Hz, 1H, 5″-H), 3.78 (dd, *J* = 6.0, 6.2 Hz, 1H, 4′-H), 4.16 (dd, *J* = 5.8, 5.9 Hz, 1H, 3′-H), 4.73 (m, 2H, 2′-H, 3′-OH), 5.11 (d, *J* = 6.1 Hz, 1H, 5′-OH), 5.32 (d, *J* = 5.3 Hz, 1H, 2′-OH), 6.30 (d, *J* = 4.0 Hz, 1H, 1′-H), 7.34 (dd, *J* = 3.9, 5.0 Hz, 1H, 4″-H), 7.77 (d, *J* = 3.3 Hz, 1H, 3″-H), 8.10 (s, 1H, =CH), 8.15 (d, *J* = 5.0 Hz, 1H, 5″-H); MS, *m/z* = 359 (M^+); Anal. Calcd. for $C_{13}H_{13}NO_5S_3$ (359.44): C, 43.44; H, 3.65; N, 3.90. Found: C, 43.53; H, 3.86; N, 3.64.

8.16. 5-((Z)-2-Furylidene)-3-(β-D-ribofuranosyl)-2-thioxo-4-thiazolidinone (10f)

Yield 260 mg (79%); yellow solid; mp 130–132 °C; IR (KBr): *ν* 3400 cm^{-1} (OH), 1672 cm^{-1} (CO), 1230 cm^{-1} (CS); ^{1}H NMR (DMSO-d_6): *δ* 3.42 (dd, *J* = 6.1, 11.9 Hz, 1H, 5′-H), 3.64 (dd, *J* = 4.9, 11.7 Hz, 1H, 5″-H), 3.74 (dd, *J* = 6.0, 6.2 Hz, 1H, 4′-H), 4.16 (dd, *J* = 5.8, 6.0 Hz, 1H, 3′-H), 4.70 (m, 2H, 2′-H, 3′-OH), 5.08 (d, *J* = 6.0 Hz, 1H, 5′-OH), 5.28 (d, *J* = 5.3 Hz, 1H, 2′-OH), 6.32 (d, *J* = 4.0 Hz, 1H, 1′-H), 6.80 (dd, *J* = 1.8, 2.8 Hz, 1H, 4″-H), 7.26 (d, *J* = 2.9 Hz, 1H, 3″-H), 7.60 (d, *J* = 1.8 Hz, 1H, 5″-H), 8.10 (s, 1H, =CH); MS, *m/z* = 343 (M^+); Anal. Calcd. for $C_{13}H_{13}NO_6S_2$ (343.38): C, 45.47; H, 3.82; N, 4.08. Found: C, 45.63; H, 4.06; N, 3.89.

Method B: To a mixture of the protected nucleoside **9** (265 mg, 1 mmol), anhydrous morpholine (0.09 g, 1 mmol) and anhydrous ethanol (10 ml) was added benzaldehyde (0.11 g, 1 mmol). The mixture was stirred until the starting material was consumed (12 h; TLC). The reaction mixture was neutralized with HCl/MeOH. After stirring for 5 min, the solution was evaporated *in vacuo* and the residue was purified by flash chromatography (eluent 30–50%, diethyl ether/petroleum ether, 40–60 °C) to afford 230 mg (87%) of **10a** as yellow solid.

8.17. 5-((Z)-Arylidene)-3-(2′,3′,4′,6′-tetra-O-acetyl-β-D-mannopyranosyl)-2-thioxo-4-thiazolidinones (13a-c)

General Procedure: 5-((Z)-Arylidene)-2-thioxo-4-thiazolidinones (**6a,b,e**) (5 mmol) was suspended in anhydrous MeCN (25 ml) at room temperature. To this suspension was added NaH (50%, 0.26 g, 5 mmol), and the mixture was stirred at room temperature for 30 min. The mixture became clear after 15 min. 2,3,4,6-tetra-*O*-acetyl-α-D-mannopyranosyl bromide (**12**) (2.26 g, 5.5 mmol) was added, and the mixture was stirred at room temperature for 12 h until the starting material was consumed (TLC) and then filtered. The residue from the evaporation of the filtrate under reduced pressure was purified by flash chromatography (eluent 30–50%, diethyl ether/petroleum ether, 40–60 °C) to afford the title compounds **13a-c**.

8.18. 5-((Z)-Benzylidene)-3-(2′,3′,4′,6′-tetra-O-acetyl-β-D-mannopyranosyl)-2-thioxo-4-thiazolidinones (13a)

Yield 1.98 g (92%); yellow solid; mp 162–164 °C; IR: *ν* 1752 cm^{-1} (CO), 1747 cm^{-1} (CO), 1240 cm^{-1} (CS); ^{1}H NMR ($CDCl_3$): *δ* 1.95 (s, 3H, Ac), 2.05 (s, 3H, Ac), 2.07 (s, 3H, Ac), 2.11 (s, 3H, Ac), 3.87–3.91 (m, 1H, 5′-H), 4.23–4.26 (m, 2H, 6′-H, 6″-H), 5.53 (dd, *J* = 9.7, 9.8 Hz, 1H, 4′-H), 5.38 (dd, *J* = 9.1, 9.5 Hz, 2′-H), 6.16 (dd, *J* = 9.2, 9.2 Hz, 3′-H), 6.35 (d, *J* = 9.4 Hz, 1H, 1′-H), 7.43–7.46 (m, 5H, Ar–H), 7.69 (s, 1H, =CH); ^{13}C NMR ($CDCl_3$): *δ* 20.38, 20.59, 20.62, 20.76 (4 Ac),

61.67 (C-6′), 67.77 (C-2′), 67.81 (C-3′), 73.27 (C-4′), 74.89 (C-5′), 81.83 (C-1′), 120.52 (=CH), 130.94 (C-5), 129.35, 130.70, 133.11, 134.11 (C–Ar), 165.86 (C-4), 169.40, 169.59, 170.10, 170.67 (4 Ac), 194.12 (C-2); MS, m/z = 551 (M^+); Anal. Calcd. for $C_{24}H_{25}NO_{10}S_2$ (551.59): C, 52.26; H, 4.57; N, 2.54. Found: C, 52.41; H, 4.80; N, 2.34.

8.19. 5-((Z)-4-Methoxybenzylidene)-3-(2′,3′,4′,6′-tetra-O-acetyl-β-D-mannopyranosyl)-2-thioxo-4-thiazolidinone (13b)

Yield 1.97 g (68%); yellow solid; mp 216–218 °C; IR: ν 1750 cm^{-1} (CO), 1746 cm^{-1} (CO), 1238 cm^{-1} (CS); ^{1}H NMR ($CDCl_3$): δ 1.94 (s, 3H, Ac), 2.04 (s, 3H, Ac), 2.07 (s, 3H, Ac), 2.10 (s, 3H, Ac), 3.86–4.28 (m, 6H, OCH_3, 5′-H, 6′-H, 6″-H), 5.30 (dd, J = 9.7, 9.8 Hz, 1H, 4′-H), 5.38 (dd, J = 9.1, 9.5 Hz, 2′-H), 6.16 (dd, J = 9.2, 9.2 Hz, 3′-H), 6.35 (d, J = 9.4 Hz, 1H, 1′-H), 7.00, 7.46 (2d, J = 8.5 Hz, 4H, Ar–H), 7.68 (s, 1H, =CH); ^{13}C NMR ($CDCl_3$): δ 20.42, 20.61, 20.64, 20.78 (4 Ac), 55.56 (OCH_3), 61.71 (C-6′), 67.82 (C-2′, C-3′), 73.36 (C-4′), 74.88 (C-5′), 81.84 (C-1′), 114.96, 117.38, 125.87, 132.89, 134.22, 161.89 (C–Ar, =CH, C-5), 166.06 (C-4), 169.42, 169.57, 170.14, 170.70 (4 Ac), 194.17 (C-2); MS, m/z = 581 (M^+); Anal. Calcd. for $C_{25}H_{27}NO_{11}S_2$ (581.61): C, 51.63; H, 4.68; N, 2.41. Found: C, 51.85; H, 4.78; N, 2.32.

8.20. 5-((Z)-2-Thienylidene)-3-(2′,3′,4′,6′-tetra-O-acetyl-β-D-mannopyranosyl)-2-thioxo-4-thiazoli-dinone (13c)

Yield: 2.00 g (72%); yellow solid; mp 148–150 °C; IR: ν 1750 cm^{-1} (CO), 1748 cm^{-1} (CO), 1236 cm^{-1} (CS); ^{1}H NMR ($CDCl_3$): δ 1.94 (s, 3H, Ac), 2.04 (s, 3H, Ac), 2.07 (s, 3H, Ac), 2.10 (s, 3H, Ac), 3.88 (m, 1H, 5′-H), 4.27 (m, 6H, 6′-H, 6″-H), 5.30 (dd, J = 9.7, 9.8 Hz, 1H, 4′-H.), 5.38 (dd, J = 9.1, 9.6 Hz, 2′-H), 6.14 (dd, J = 9.1, 9.3 Hz, 3′-H), 6.32 (d, J = 9.3 Hz, 1H, 1′-H), 7.20 (dd, J = 0.3.8, 5.0 Hz, 1H, 4″-H), 7.42 (d, J = 3.7 Hz, 1H, 3″-H), 7.72 (d, J = 5.0 Hz, 1H, 5″-H), 7.89 (s, 1H, =CH); ^{13}C NMR ($CDCl_3$): δ 20.40, 20.60, 20.63, 20.77 (4 Ac), 61.69 (C-6′), 67.80 (C-2′, C-3′), 73.31 (C-4′), 74.89 (C-5′), 81.93 (C-1′), 118.50 (=CH), 126.39 (C-5), 129.00, 133.21, 134.33, 137.83 (C–Ar), 165.66 (C-4), 169.42, 169.58, 170.13, 170.70 (4 Ac), 193.35 (C-2); MS, m/z = 557 (M^+); Anal. Calcd. for $C_{22}H_{23}NO_{10}S_3$ (557.62): C, 47.39; H, 4.16; N, 2.51. Found: C, 47.62; H, 4.38; N, 2.30.

8.21. 5-((Z)-Arylidene)-3-(β-D-mannopyranosyl)-2-thioxo-4-thiazolidinones (14a,b)

General Procedure: The protected nucleosides **13a,b** (1 mmol) were suspended in MeOH (15 ml), and concentrated HCl (0.5 ml) was added. The reaction mixture was heated for 2 h at 50 °C. To the resulting solution was added an ion exchange resin (Amberlite IR-120, OH^--form), previously washed with MeOH. After stirring for 5 min, the solution was filtered and evaporated *in vacuo* and the residue was purified by flash chromatography (eluent 0–5%, $CHCl_3$/MeOH) to afford the title compounds **14a,b**.

8.22. 5-((Z)-Benzylidene)-3-β-D-mannopyranosyl-2-thioxo-4-thiazolidinone (14a)

Yield: 306 mg (80%); yellow solid; mp 148–150 °C; IR (KBr): ν 3392 cm^{-1} (OH), 1718 cm^{-1} (CO), 1225 cm^{-1} (CS); ^{1}H NMR (CD_3OD-d_4): δ 3.22 (m, 1H, 4′-H), 3.34 (m, 3H, 5′-H, 6′-H, 6″-H), 3.60 (m, 1H, 3′-H), 3.82 (m, 1H, 2′-H), 6.00 (d, J = 9.4 Hz, 1H, 1′-H), 7.32–7.48 (m, 5H, Ar–H), 7.60 (s, 1H, =CH); ^{13}C NMR (CD_3OD-d_6): δ 62.74 (C-6′), 69.43 (C-2′), 71.30 (C-3′), 79.16 (C-4′), 81.50 (C-5′), 86.02 (C-1′), 122.53 (=CH), 127.24 (C-5), 130.47, 131.70, 131.81, 131.92, 133.81, 134.65 (C–Ar), 168.15 (C-4), 196.85 (C-2); MS, m/z = 383 (M^+); Anal. Calcd. for $C_{16}H_{17}NO_6S_2$ (383.44): C, 50.12; H, 4.47; N, 3.65. Found: C, 50.36; H, 4.67; N, 3.45.

8.23. 5-((Z)-4-Methoxybenzylidene)-3-(β-D-mannopyranosyl)-2-thioxo-4-thiazolidinone (14b)

Yield: 351 mg (85%); yellow solid; mp 136–138 °C; IR (KBr): ν 3396 cm^{-1} (OH), 1717 cm^{-1} (CO), 1226 cm^{-1} (CS); ^{1}H NMR (DMSO-d_6): δ 3.13–3.46 (m, 4H, 6′-H, 6′-H, 5′-H, 4′-H), 3.70 (m, 1H, 3′-H), 3.85 (s, 3H, OCH_3), 4.42 (m, 1H, 2′-H), 4.62 (s, 1H, 6′-OH), 5.10 (s, 1H, 4′-OH), 5.22 (s, 1H, 3′-OH), 5.42 (s, 1H, 2′-OH), 5.86 (d, J = 9.2 Hz, 1H, 1′-H), 7.11, 7.60 (2d, J = 8.6 Hz, 4H, Ar–H), 7.67 (s, 1H, =CH); ^{13}C NMR (DMSO-d_6): δ 55.62 (OCH_3), 61.15 (C-6′), 67.68 (C-2′), 69.94 (C-3′), 77.60 (C-4′), 80.78 (C-5′), 84.98 (C-1′), 117.63 (=CH), 120.81 (C-5), 115.17, 125.57, 132.89, 161.60 (C–Ar), 166.16 (C-4), 195.26 (C-2); MS, m/z = 413 (M^+); Anal. Calcd. for $C_{17}H_{19}NO_7S_2$ (413.47): C, 49.38; H, 4.63; N, 3.39. Found: C, 49.53; H, 4.80; N, 3.14.

9. Computational details

The molecular structures of the investigated compounds were optimized using DFT (density functional theory) in combination with the Beck's three parameter exchange functional along with the Lee-Yang-Parr non local correlation functional (B3LYP) [54–56] with 6-31 + G(d) basis set which is implemented in Gaussian 09 program package [57]. An estimate of molecular properties related to molecular reactivity was calculated with DFT/B3LYP combination [58]. The molecular properties include the highest occupied molecular orbital (HOMO), the lowest unoccupied molecular orbital (LUMO), global hardness and softness, electronegativity, electron affinity, ionization potential, etc [31,59–61].

10. Shape alignment and ROCS [51–53]

Basic method to represent shape and color features in ROCS is using ROCs application Open Eye scientific software. BTR1 and GSK were selected as query molecules. Compounds library was adopted as the database file. Both query and database files were energy minimized by Omega applications. ROCS runs were employed by personal PC in very fast using vROCS interface. vROCS was employed to run and analyze/visualize the results. ROCS application searched the database with the query to find molecules with similar shape and colors. Compounds conformers were scored based upon the Gaussian overlap to the query and the best scoring parameters is Tanimoto Combo scores (shape + color), the highest score is the best matched with query compound.

Declaration of competing interest

There is no conflict of interest between the Authors.

Acknowledgements

We thank ADIR (*Groupe Servier, paris*) for carrying out the antitumor testing of the prepared new deprotected nucleosides. Ahmed I. Khodair is grateful for an Alexander von Humboldt-Fellowship.

Appendix A. Supplementary data

Supplementary data to this article can be found online at https://doi.org/10.1016/j.carres.2019.107894.

References

[1] T. Tomasic, L.P. Masic, Rhodanine as a privileged scaffold in drug discovery, Curr. Med. Chem. 16 (2009) 1596–1629, https://doi.org/10.2174/092986709788186200.
[2] T. Tomasic, L.P. Masic, Rhodanine as a scaffold in drug discovery: a critical review

of its biological activities and mechanisms of target modulation, Expert Opin. Drug Discov. 7 (2012) 549–560, https://doi.org/10.1517/17460441.2012.688743.
[3] P. Hirsova, J. Dolezel, M. Kucerova-Chlupacova, J. Kunes, V. Pilarova, L. Novakova, v. Opletalova, (Z)-3-amino-5-(pyridin-2-ylmethylidene)-2-thioxo-1,3thiazolidin-4-one, Molbank 4 (2015) M872, https://doi.org/10.3390/M872.
[4] J. Dolezel, V. Opletalova, M. Vejsova, P. Hirsova, Evaluation of thiazolidine derivatives, abstracts of the 5th international postgraduate research symposium on pharmaceutics (IPORSIP2007), istanbul, Turkey, 13–15 september 2007, Acta Pharm. Sci. 49 (2007) 31–43 ([Google scholar]).
[5] P. Petrik, J. Kunes, M. Vejsova, J. Jampilek, E. Spaningerova, D. Kesetovicova, M. Vlckova, M. Majd, S. Kalafutova, V. Opletalova, Antifungal and anti-mycobacterial properties of 5-arylmethylidenerhodanines and their N_3-substituted analogues, abstracts of the 5th international postgraduate research symposium on pharmaceutics (IPORSIP-2007), istanbul, Turkey, 13–15 september 2007, Acta Pharm. Sci. 49 (2007) 77–87 ([Google scholar]).
[6] J. Dolezel, P. Hirsova, V. Opletalova, J. Dohnal, M. Vejsova, J. Kunes, J. Jampilek, Rhodanineacetic acid derivatives as potential drugs: preparation, hydrophobic properties and antifungal activity of (5-arylalkylidene-4-oxo-2-thioxo-1,3-thiazolidin-3-yl)acetic acids, Molecules 14 (2009) 4197–4212, https://doi.org/10.3390/molecules14104197.
[7] V. Opletalova, J. Dolezel, V. Buchta, M. Vejsova, P. Paterova, Antifungal effects of (5Z)-5-arylmethylidenerhodanines with a special view to members of mucorales, Folia Pharm. Univ. Carol. 42 (7–13) (2014) ([Google scholar]).
[8] V. Opletalova, J. Dolezel, K. Kralova, M. Pesko, J. Kunes, J. Jampilek, Synthesis and characterization of (Z)-5-arylmethylidenerhodanines with photosynthesis-inhibiting properties, Molecules 16 (2011) 5207–5227, https://doi.org/10.3390/molecules16065207.
[9] Y. Ohishi, T. Mukai, M. Nagahara, M. Yajima, N. Kajikawa, K. Miyahara, T. Takano, Preparations of 5-alkylmethylidene-3-carboxymethylrhodanine derivatives and their aldose reductase inhibitory activity, Chem. Pharm. Bull. 38 (1990) 1911–1919, https://doi.org/10.1248/cpb.38.1911.
[10] Y. Momose, K. Meguro, H. Ikeda, C. Hatanaka, S. Oi, T. Sohda, Studies on antidiabetic agents X: synthesis and biological activities of pioglitazone and related compounds, Chem. Pharm. Bull. 39 (1991) 1440–1445, https://doi.org/10.1248/cpb.39.1440.
[11] K. Sudo, Y. Matsumoto, M. Matsushima, M. Fujiwara, K. Konno, K. Shimotohno, S. Shigeta, T. Yokota, novel hepatitis C virus protease inhibitors: thiazolidine derivative, Biochem. Biophys. Res. Commun. 238 (1997) 643–647, https://doi.org/10.1006/bbrc.1997.7358.
[12] M.M. Sim, S.B. Ng, A.D. Buss, S.C. Crasta, K.L. Goh, S.K. Lee, Rhodanines as novel inhibitors of UDP-N-acetylmuramate/L-alanine ligase, Bioorg. Med. Chem. Lett 12 (2002) 697–699, https://doi.org/10.1016/S0960-894X(01)00832-0.
[13] R. Frlan, A. Kovac, D. Blanot, S. Gobec, S. Pecar, A. Obreza, Design and synthesis of novel *N*-benzylidenesulfonohydrazide inhibitors of MurC and MurD as potential antibacterial agents, Molecules 13 (2008) 11–30, https://doi.org/10.3390/molecules13010011.
[14] K. Kristan, M. Kotnik, M. Oblak, U.J. Urleb, New high-throughput fluorimetric assay for discovering inhibitors of UDP-N-acetylmuramyl-L-alanine: D-glutamate (MurD) ligase, Biomol. Screen. 14 (2009) 412–418, https://doi.org/10.1177/1087057109332597.
[15] B. Bulic, M. Pickhardt, I. Khilstunova, J. Biernat, E.M. Mandelkow, E. Mandelkow, H. Waldmann, Rhodanine-based tau aggregation inhibitors in cell models of tauopathy, Angew. Chem. Int. Ed. 46 (2007) 9215–9219, https://doi.org/10.1002/anie.200704051.
[16] E. Zeiger, B. Anderson, S. Haworth, T. Lawlor, W. Mortelmans, Salmonella mutagenicity tests: III. Results from the testing of 255 chemicals, Environ. Mutagen. 9 (1987) 1–109, https://doi.org/10.1002/em.2860090602.
[17] N. Hotta, Long-term clinical effects of epalrestat, an aldose reductase inhibitor, on diabetic peripheral neuropathy: the 3-year, multicenter, comparative aldose reductase inhibitor-diabetes complications trial, Diabetes Care 29 (2006) 1538–1544, https://doi.org/10.2337/dc05-2370.
[18] B.T. Moorthy, S. Ravi, M. Srivastava, K. K, S.C. Chiruvella, Novel rhodanine derivatives induce growth inhibition followed by apoptosis, Med. Chem. Lett. 20 (2010) 6297–6301, https://doi.org/10.1016/j.bmcl.2010.08.084.
[19] M. Azizmohammadi, M. Khoobi, A. Ramazani, S. Emami, 2H-chromene derivatives bearing thiazolidine-2,4-dione, rhodanine or hydantoin moieties as potential anticancer agents, Eur. J. Med. Chem. 59 (2013) 15–22, https://doi.org/10.1016/j.ejmech.2012.10.044.
[20] S.P. Mandal, A. Garg, S.S. Sahetya, S.R. Nagendra, H.S. Sripad, M.M. Manjunath, Sitaram, M. Soni, R.N. Baig, S.V. Kumarc, B.R.P. Kumar, Novel rhodanines with anticancer activity: design, synthesis and CoMSIA study, RSC Adv. 6 (2016) 58641–58653, https://doi.org/10.1039/c6ra08785j.
[21] R. Kumar, J.W. Lown, Synthesis and antitumor cytotoxicity evaluation of novel thiazole-containing glycosylated polyamides, Eur. J. Org. Chem. 24 (2003) 4842–4851, https://doi.org/10.1002/ejoc.200300532.
[22] S.D. Knight, N.D. Adams, J.L. Burgess, A.M. Chaudhari, M.G. Darcy, C.A. Donatelli, J.I. Luengo, K.A. Newlander, C.A. Parrish, L.H. Ridgers, M.A. Sarpong, S.J. Schmidt, G.S. Van Aller, J.D. Carson, M. Diamond, A.P.A. Elkins, C.M. Gardiner, E. Garver, S.A. Gilbert, R.R. Gontarek, J.R. Jackson, K.L. Kershner, L. Luo, K. Raha, C.S. Sherk, C.M. Sung, D. Sutton, P.J. Tummino, K.R.W. grzyn, R. J Auger, D. Dhanak, Discovery of GSK2126458, a highly potent inhibitor of PI3K and the mammalian target of rapamycin, ACS Med. Chem. Lett. 1 (2010) 39–43, https://doi.org/10.1021/ml900028r.
[23] A.A. El-Barbary, A.I. Khodair, E.B. Pedersen, C. Nielsen, S-glucosylated hydantoins as new antiviral agents, J. Med. Chem. 37 (1994) 73–77, https://doi.org/10.1021/jm00027a009.
[24] A.I. Khodair, H.I. EL-Subagh, A.A. El-Emam, Synthesis of certain 5-substituted 2-thiohydantoin derivatives as potential cytotoxic and antiviral agents, Boll. Chim. Farm. 136 (1997) 561–567 [PMID: 9440349].
[25] A.M. Al-Obaid, H.I. EL-Subagh, A.I. Khodair, M.M.A. Elmazar, 5-substituted-2-thiohydantoin analogs as a novel class of antitumor agents, Anti Canccer Drugs 7 (1996) 873–880, https://doi.org/10.1097/00001813-199611000-00009.
[26] A.I. Khodair, Glycosylation of 2-thiohydantoin derivatives, synthesis of some novel s-alkylated and s-glucosylated hydantoins, Carbohydr. Res. 331 (2001) 445–453, https://doi.org/10.1016/S0008-6215(01)00040-4.
[27] A.I. Khodair, Synthesis of 2-thiohydantoins and their S-glucosylated derivatives as potential antiviral and antitumor agents, Nucleosides Nucleotides Nucleic Acids 20 (2001) 1735–1750, https://doi.org/10.1081/NCN-100105908.
[28] K.N. Houk, F. Liu Holy, Holy grails for computational organic chemistry and biochemistry, Acc. Chem. Res. 50 (2017) 539–543, https://doi.org/10.1021/acs.accounts.6b00532.
[29] M.M. Kabanda, L.C. Murulana, M. Ozcan, F. Karadag, Quantum chemical studies on the corrosion inhibition of mild steel by some triazoles and benzimidazole derivatives in acidic medium, Int. J. Electrochem. Sci. 7 (2012) 5035–5056 ([Google Scholar]).
[30] P. Udhayakala, A. Jayanthi, T.V. Rajendiran, Adsorption and quantum chemical studies on the inhibition potentials of some formazan derivatives, Der Pharma Chem. 3 (2011) 528–539 ([Google Scholar]).
[31] M.K. Awad, M.S. Masoud, M.A. Shaker, A.E. Ali, MP2 and DFT theoretical studies of the geometry, vibrational and electronic absorption spectra of 2-aminopyrimidine, Res. Chem. Intermed. 39 (2013) 2741–2761, https://doi.org/10.1007/s11164-012-0795-3.
[32] F.M. Atlam, M.K. Awad, E.A. El-bastawissy, Computational simulation of the effect of quantum chemical parameters on the molecular docking of HMG-CoA reductase drugs, J. Mol. Struct. 1075 (2014) 311–326, https://doi.org/10.1016/j.molstruc.2014.06.045.
[33] A.I. Khodair, A.M. Attia, E.A. Gendy, Y.A.M.M. Elshaier, M.A. El-Magd, Design, synthesis and cytotoxicity evaluation of some novel *S*-glycoside of 2-thioxopyridine and *N*-glycoside of 2-oxopyridine derivatives as antibreast cancer, J. Heterocycl. Chem. 56 (2019) 1733–1747, https://doi.org/10.1002/jhet.3527.
[34] A.M. Attia, A.I. Khodair, E.A. Gendy, M.A. El-Magd, Y.A.M.M. Elshaier, New 2-oxopyridine/2-thiopyridine derivatives tethered to a benzotriazole with cytotoxicity on MCF7 cell lines and with antiviral activities, Lett. Drug Des. Discov. 16 (2019) 1–14, https://doi.org/10.2174/1570180816666190220123547.
[35] L.M. Werbel, N. Headen, E.F. Elslager, 3-phenylrhodanines as potential antimalarial agents, J. Med. Chem. 11 (1968) 364–365, https://doi.org/10.1021/jm00308a040.
[36] F.C. Brown, C.K. Bradsher, S.M. Bond, R.J. Granthan, Mildew-preventing activity of rhodanine derivatives, Ind. Eng. Chem. 46 (1954) 1508–1512, https://doi.org/10.1021/ie50535a054.
[37] H. Vorbruggen, K. Krolikiewicz, B. Bennua, Nucleoside syntheses XXII: nucleoside synthesis with trimethylsilyl triflate and perchlorate as catalysts, Chem. Ber. 114 (1981) 1234–1255, https://doi.org/10.1002/cber.19811140404.
[38] A.I. Khodair, Convenient synthesis of 2-arylidene-5*H*-thiazolo[2,3-*b*]quinazoline-3,5[2*H*]-diones and their benzoquinazoline derivatives, J. Heterocycl. Chem. 39 (2002) 1153–1160, https://doi.org/10.1002/jhet.5570390607.
[39] U. Piantini, O.W. Sorensen, R.R. Ernst, Multiple quantum filters for elucidating NMR coupling networks, J. Am. Chem. Soc. 104 (1982) 6800–6801, https://doi.org/10.1021/ja00388a062.
[40] A.A. Bothner-By, R.L. Stephensen, J. Lee, C.D. Warren, R.W. Jeanloz, Structure determination of tetrasaccharide: transient nuclear overhauser effects in the rotating frame, J. Am. Chem. Soc. 106 (1984) 811–813, https://doi.org/10.1021/ja00315a069.
[41] A. Bax, D.G. Davis, Practical aspects of two-dimensional transverse NOE spectroscopy, J. Magn. Reson. 63 (1985) 207–213 ([Google Scholar]).
[42] C. Griesinger, R.R. Ernst, Frequency offset effects and their elimination in NMR rotating-frame cross-relaxation spectroscopy, J. Magn. Reson. 75 (1987) 261–271, https://doi.org/10.1016/0022-2364(87)90035-7.
[43] G. Gosselin, H.F. Loukil, A. Mathieu, A. Mesli, J.L. Imbach, Ribosylation of various 2-mercaptobenzoazole, J. Heterocycl. Chem. 15 (1978) 657–664, https://doi.org/10.1002/jhet.5570150427.
[44] N.A. Al-Masoudi, Y.A. Al-Soud, A. Geyer, ^{1}H- and ^{13}C-NMR study of some 6,7- dihaloquinolone nucleosides and their derivatives, Spectrosc. Lett. 31 (1998) 1031–1038, https://doi.org/10.1080/00387019808003281.
[45] D. Villemin, A.B. Alloun, Synthesis of α-thioacrylic acids and phosphonothionothiazolidinones, phosphorus, sulfur, silicon and reat, Elmen 79 (1993) 33–41, https://doi.org/10.1080/10426509308034395.
[46] A.A. El-Barbary, A.I. Khodair, E.B. Pedersen, C. Nielsen, Synthesis of uridine with 5-methylene-2-thiohydantoin substituent in the 5-position, Liebigs Ann. Chem. (1994) 619–621, https://doi.org/10.1002/jlac.199419940613.
[47] T. Ishida, Y. In, M. Inoue, Y. Ueno, C. Tanaka, Structural elucidation of epalrestat (ONO-2235), a potent aldose reductase inhibitor, and isomerization of its double bonds, Tetrahedron Lett. 30 (1989) 959–962, https://doi.org/10.1016/S0040-4039(00)95290-0.
[48] R.U. Lemieu, Reactions of carbohydrates, Methods Carbohydr. Chem. 2 (1963) 221–222 ([Google Scholar]).
[49] A.I. Khodair, J.P. Gesson, A new approach for the N-galactosylation and S-galactosylation of 5-arylidene-2-thioxo-4-thiazolidinones, Carbohydr. Res. 364 (2011) 2831–2837, https://doi.org/10.1016/j.carres.2011.09.035.
[50] A. Monks, D. Scudiero, P. Skehan, R. Shoemaker, K. Poull, D. Vistica, C. Hose, J. Langly, P. Cronise, A. Viagro-Wolff, M. Gray-Goodrish, H. Compell, M.J. Boyd, Feasibility of a high-flux anticancer drug screen using a diverse panel of cultured human tumor cell lines, J. Natl. Cancer Inst. 83 (1991) 757–766, https://doi.org/

10.1093/jnci/83.11.757.
[51] ROCS, version 2.5.1.4; OpenEye http://www.openey.com.
[52] VIDA, version 4.1.2, OpenEye Scientific software, santa Fe, NM (USA), http://www.eyesopen.com.
[53] K.R.A. Abdellatif, W.A.A. Fadaly, G.M. Kamel, Y.A.M.M. Elshaier, M.A. El-Magd, design, synthesis, modeling studies and biological evaluation of thiazolidine derivatives containing pyrazole core as potential anti-diabetic PPAR-γ agonists and anti-inflammatory COX-2 selective inhibitors, Bioorg. Chem. 82 (2019) 86–99, https://doi.org/10.1016/j.bioorg.2018.09.034.
[54] A.D. Becke, Density-functional thermochemistry II: the effect of the Perdew-Wang generalized-gradient correlation correction, J. Chem. Phys. 97 (1992) 9173–9177, https://doi.org/10.1063/1.463343.
[55] A.D. Becke, A new mixing of Hartree–Fock and local density-functional theories, J. Chem. Phys. 98 (1993) 1372–1377, https://doi.org/10.1063/1.464304.
[56] C. Lee, W. Yang, R.G. Parr, Development of the colle-salvetti correlation-energy formula into a functional of the electron density, Phys. Rev. B. 37 (1988) 785–789, https://doi.org/10.1103/PhysRevB.37.785.
[57] M.J. Frisch, Gaussian 09, Revision B.01, Gaussian, Inc., Pittsburgh, (2009) https://gaussian.com/g09citation/.
[58] P. Senet, Letters, chemical harnesses of atoms and molecules from frontier orbitals, Chem. Phys. Lett. 275 (1997) 527–532, https://doi.org/10.1016/S0009-2614(97)00799-9.
[59] W. Langenaeker, P. Geerlings, F. De Proft, Theory, conceptual density functional, Chem. Rev. 103 (2003) 1793–1874, https://doi.org/10.1021/cr990029p.
[60] S.L. PU, Materials for nonlinear optics-chemical perspectives, chapter 22: observing high second harmonic generation and control of molecular alignment in one dimension, ACS Symp. Ser. 455 (1991) 331–342 ([Google Scholar]).
[61] E. Scrocco, J. Tomasi, Electronic molecular structure, reactivity and intermolecular forces: an euristic interpretation by means of electrostatic molecular potentials, Adv. Quant. Chem. 11 (1978) 115–193, https://doi.org/10.1016/S0065-3276(08)60236-1.